Algebraic Input-output Angle Equation Derivation Algorithm for the Six Distinct Angle Pairings in Arbitrary Planar 4R Linkages

Mirja Rotzoll[1], Quinn Bucciol[2], and M. John D. Hayes[3]

Abstract— **This paper describes a generalised algorithm that can be applied to any single degree of freedom parallel kinematic chain to determine the algebraic polynomial that represents the input-output equation relating any pair of distinct angles between any pair of links in the kinematic chain. There are six such algebraic polynomials for an arbitrary four-bar linkage. The algorithm consists of assigning standard Denavit-Hartenberg coordinate systems and parameters to the open kinematic chain. The open chain is conceptually closed by equating the forward kinematic transformation that maps coordinates of points in the "end-effector" coordinate system to the relatively non-moving base coordinate system to the identity matrix. The resulting transformation is mapped to Study soma coordinates wherein the twist and joint angles have been converted to tangent half-angle parameters. Elimination theory is then applied to the soma coordinates revealing a single algebraic polynomial in terms of the link lengths and the desired angle pair. Example applications are discussed for continuous approximate synthesis, mobility classification, and the design parameter space.**

I. INTRODUCTION

Parallel kinematic chains have fascinated kinematicians for thousands of years [1]. Even the humble planar four-bar kinematic chain has been the focus of intense research for at least as long. Ever since humans had the ability to formulate abstract thoughts, for countless thousands of years, four-bar linkages, in their many forms, have been used to perform a large variety of tasks everywhere there have been human beings [2]. The science of mechanisms has evolved such that now nearly every article of clothing you wear, the vehicles you are transported by, the household devices you use, even the streets you walk upon have all been touched by at least one, or two, if not many thousands, of four-bar linkages. The literature is rich with many recent results investigating function and coupler curve generation together with motion generation problems, differential kinematics, and force and torque transfer. Results reported in [3], [4], [5], [6], [7], [8] are a small, but broad sampling. Given such current interest, we feel justified to continue identifying new and useful methods for analysis and synthesis of parallel kinematic chains in general, but of planar 4R linkages in particular.

[1]Ph.D. Candidate, Department of Mechanical and Aerospace Engineering, Carleton University, Ottawa, ON, Canada, mirja.rotzoll@carleton.ca

[2]Undergraduate Student, Department of Mechanical and Aerospace Engineering, Carleton University, Ottawa, ON, Canada, quinn.bucciol@carleton.ca

[3]Professor, Department of Mechanical and Aerospace Engineering, Carleton University, Ottawa, ON, Canada, john.hayes@carleton.ca

In this paper we present a novel algorithm, built on tools from algebraic-geometry, that derives the algebraic polynomial which models the relative displacements of one of six desired input-output angle pairs in an arbitrary single degree of freedom 4R simple closed kinematic chain. First, the class of planar 4R open kinematic chains is parameterised using the well known notation for lower-pair kinematic chains of arbitrary architecture, known as Denavit-Hartenberg (DH) notation [9]. The resulting coordinate transformation matrix describing the forward kinematics of the open chain is equated to the identity matrix to conceptually close the chain [9]. Measures of angle elements in the resulting matrix are converted to their respective tangent half-angle parameters. This modified transformation matrix is then mapped to the coordinates of the seven dimensional projective kinematic image space using the well known definitions of the Study soma coordinates [10], [11], [12], [13]. Next, using an appropriate subset of the soma coordinates, elimination theory [14] is used to eliminate undesired variable angle parameters leaving only the desired input-output (IO) angle parameter pair algebraic equation. The first presentation of a part of the algorithm can be found in [15]. However, in that work we failed to understand how completely general the algorithm is and this work will serve to correct that. While we have successfully applied the algorithm to derive the input-output angles for all planar, spherical, and some spatial four-bar linkages [16], [17], we will present only the results for the class of planar 4R linkages.

The motivation at the foundation of this work is to provide computational tools for mechanism design and analysis that are less cumbersome to use than vector loop methods based on trigonometry. Since our IO equations are algebraic polynomials of degree 4 in two variables with rational coefficients, the full power of the theory of planar algebraic curves [18] can be applied to the six distinct IO degree 4 algebraic IO curves allowing for significantly more and comparatively simple to obtain information regarding the relative motions generated by the linkage.

II. DEFINING THE KINEMATIC GEOMETRY

We start with a generic 4R open kinematic chain and assign the standard DH coordinate systems and parameters according to [9], see Table I and Fig. 1 The four link lengths are the a_i, and the four joint angles are the θ_i, $i \in \{1, 2, 3\}$. The transformation matrix implied by these parameters is equated to the identity matrix thereby conceptually closing the kinematic chain. But, this process means that the coordinate system that moves with link a_4 aligns out of

phase by π radians with the x_0 basis vector illustrated in Fig. 1. The $x_{0/4}$ - $y_{0/4}$ coordinate system illustrated in Fig. 2 is therefore used for the relatively non-moving reference coordinate system. The equations that follow are derived in that coordinate system.

TABLE I
DH PARAMETERS FOR AN ARBITRARY OPEN 4R CHAIN.

axis i	link length a_i	angle θ_i	link offset d_i	twist τ_i
1	a_1	θ_1	0	0
2	a_2	θ_2	0	0
3	a_3	θ_3	0	0
4	a_4	θ_4	0	0

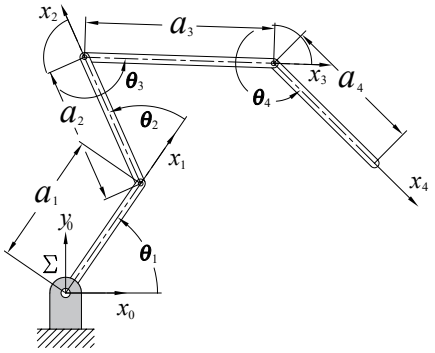

Fig. 1. Generic open 4R kinematic chain.

Using the definitions found in [15], the DH transformation matrix is mapped to the soma array of eight coordinates

$$[x_0 : x_1 : x_2 : x_3 : y_0 : y_1 : y_2 : y_3].$$

However, because we are only considering planar Euclidean displacements, the same four soma coordinates always vanish for the planar 4R and what remains are

$$[x_0 : 0 : 0 : x_3 : 0 : y_1 : y_2 : 0]. \tag{1}$$

For a generic representation, however, we use the full Study array here since the 0 elements are different for spherical and spatial linkages [16], [17].

Let the input angle parameter be v_1 and the output angle parameter be v_4. Applying two elimination steps to the three equations represented by the soma coordinates x_3, y_1 and y_2 to eliminate the angle parameters v_2 and v_3 from the equations yields the algebraic IO equation relating the v_1 and v_4 angle parameters, which we call the v_1-v_4 IO equation. It has the form

$$Av_1^2v_4^2 + Bv_1^2 + Cv_4^2 - 8a_1a_3v_1v_4 + D = 0, \tag{2}$$

where

$$\begin{aligned}
A &= A_1A_2 = (a_1 - a_2 + a_3 - a_4)(a_1 + a_2 + a_3 - a_4),\\
B &= B_1B_2 = (a_1 + a_2 - a_3 - a_4)(a_1 - a_2 - a_3 - a_4),\\
C &= C_1C_2 = (a_1 - a_2 - a_3 + a_4)(a_1 + a_2 - a_3 + a_4),\\
D &= D_1D_2 = (a_1 + a_2 + a_3 + a_4)(a_1 - a_2 + a_3 + a_4),\\
v_1 &= \tan\tfrac{\theta_1}{2},\\
v_4 &= \tan\tfrac{\theta_4}{2}.
\end{aligned}$$

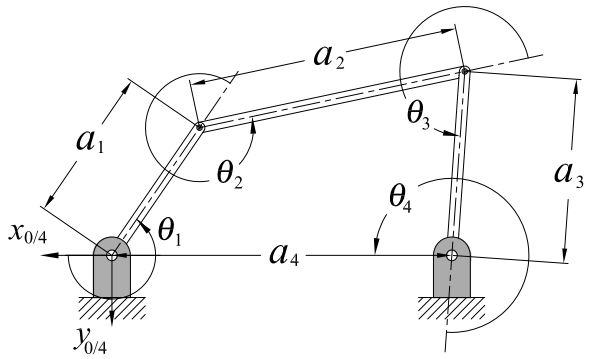

Fig. 2. Generic closed 4R kinematic chain.

This algebraic equation is of degree four in the v_1 and v_4 variable parameters, while the coefficients labelled A, B, C, and D are products of bilinear factors which can be viewed as eight distinct planes treating the four a_i link lengths as homogeneous coordinates.

The two elimination steps are two applications of the Buchberger algorithm [19] using two different monomial orders for multivariate polynomials. The first application applies the graded reverse lexicographic order to the variables ordered as $v_3 < v_2 < v_1 < v_4$, and the second application uses the pure lexicographic order such that $v_3 > v_2 > v_1 > v_4$. This leads to a single Gröbner basis equation in the link lengths a_1, a_2, a_3, a_4 and the joint angle parameters v_1 and v_4, namely Eq. (2). Note that resultants could also be employed using Sylvester's matrix, but this method frequently results in spurious factors.

The remaining five IO quartic algebraic equations for the other distinct angle pairings all contain all eight of the bilinear factors of the coefficients labelled $A_1, A_2, B_1, B_2, C_1, C_2, D_1$, and D_2 but in different arrangements. This means that the design parameter space, as defined in [20], is the same for all six of these IO equations.

By applying the monomial term orderings to the variables in the appropriate sequence, the v_1-v_2, v_1-v_3, v_2-v_3, v_2-v_4, and v_3-v_4 IO equations are obtained and listed as follows.

$$A_1B_2v_1^2v_2^2 + A_2B_1v_1^2 + C_1D_2v_2^2 - 8a_2a_4v_1v_2 + C_2D_1 = 0, \tag{3}$$

$$A_1B_1v_1^2v_3^2 + A_2B_2v_1^2 + C_2D_2v_3^2 + C_1D_1 = 0, \tag{4}$$

$$A_1D_2v_2^2v_3^2 + B_2C_1v_2^2 + B_1C_2v_3^2 - 8a_1a_3v_2v_3 + A_2D_1 = 0, \tag{5}$$

$$A_1C_1v_2^2v_4^2 + B_2D_2v_2^2 + A_2C_2v_4^2 + B_1D_1 = 0, \tag{6}$$

$$A_1C_2v_3^2v_4^2 + B_1D_2v_3^2 + A_2C_1v_4^2 + 8a_2a_4v_3v_4 + B_2D_1 = 0. \tag{7}$$

Each of these six IO equations is of degree 4 in the two variable angle parameters, thereby defining a curve of degree 4 in the plane spanned by the different v_i-v_j angle parameter pairs. They also all have genus 1 allowing a maximum number of two assembly modes. The similar form of Eqs (2), (3), (5), and (7) arises because they relate adjacent angle pairs, while Eqs (4) and (6) relate opposite angle pairs.

III. Applications

Aside from position analysis, we will consider several important applications that these algebraic polynomials naturally and easily lend themselves to which are otherwise not generally possible using traditional vector loops and trigonometry.

A. Continuous Approximate Dimensional Synthesis

Because we have expressions for the six distinct angular relationships between the four quadrangle edges of the planar 4R, we can generate six distinct functions. It may also be that we can synthesise a linkage to generate more than one function between different links. Imagine a manufacturing and assembly operation where a single four-bar can perform multiple tasks over different angular ranges as the linkage moves. However, here we will restrict ourselves to dimensional synthesis generating a single desired function using the continuous approximate algorithm in [21]. This algorithm integrates the desired function between the lower and upper angular range limits thereby generating a continuous infinite set of input and output angular pairs.

The v_1-v_3 IO equation essentially relates the input angle parameter to a measure of the transmission angle. We begin by squaring Eq. (4) to eliminate the residual error values that are equal in magnitude yet opposite in sense. We partition the result into a 9x1 array of angle parameters and a 9x1 array of associated link length coefficients. The Euclidean inner products of these two arrays leads to the square of Eq. (4). The array of angle parameters is used to generate the synthesis equations.

$$\mathbf{s}_{v_1,v_3} \;=\; [v_1^4v_3^4, v_1^4v_3^2, v_1^4, v_1^2v_3^4, v_1^2v_3^2, v_1^2, v_3^4, v_3^2, 1]^T, \quad (8)$$

while the array of link lengths has the following 9 elements, which are scaled by the v_1-v_3 elements

$$a_4^4 - 4a_1a_4^3 + (6a_1^2 - 2a_2^2 + 4a_2a_3 - 2a_3^2)a_4^2 - 4a_1a_4(a_1 + a_2 - a_3)(a_1 - a_2 + a_3) + (a_1 + a_2 - a_3)^2(a_1 - a_2 + a_3)^2, \quad (9)$$

$$2a_4^4 - 8a_1a_4^3 + (12a_1^2 - 4a_2^2 - 4a_3^2)a_4^2 - 8a_1a_4(a_1^2 - a_2^2 - a_3^2) + 2(a_1 - a_2 + a_3)(a_1 + a_2 + a_3)(a_1 - a_2 - a_3)(a_1 + a_2 - a_3), \quad (10)$$

$$a_4^4 - 4a_1a_4^3 + (6a_1^2 - 2a_2^2 - 4a_2a_3 - 2a_3^2)a_4^2 - 4a_1a_4(a_1 + a_2 + a_3)(a_1 - a_2 - a_3) + (a_1 + a_2 + a_3)^2(a_1 - a_2 - a_3)^2, \quad (11)$$

$$2a_4^4 + (-4a_1^2 - 4a_2^2 + 8a_2a_3 - 4a_3^2)a_4^2 + 2(a_1 + a_2 - a_3)^2(a_1 - a_2 + a_3)^2, \quad (12)$$

$$4a_4^4 + (-8a_1^2 - 8a_2^2 - 8a_3^2)a_4^2 + 4(a_1 - a_2 + a_3)(a_1 + a_2 + a_3)(a_1 - a_2 - a_3)(a_1 + a_2 - a_3), \quad (13)$$

$$2a_4^4 + (-4a_1^2 - 4a_2^2 - 8a_2a_3 - 4a_3^2)a_4^2 + 2(a_1 + a_2 + a_3)^2(a_1 - a_2 - a_3)^2, \quad (14)$$

$$a_4^4 + 4a_1a_4^3 + (6a_1^2 - 2a_2^2 + 4a_2a_3 - 2a_3^2)a_4^2 + 4a_1(a_1 + a_2 - a_3)(a_1 - a_2 + a_3)a_4 + (a_1 + a_2 - a_3)^2(a_1 - a_2 + a_3)^2, \quad (15)$$

$$2a_4^4 + 8a_1a_4^3 + (12a_1^2 - 4a_2^2 - 4a_3^2)a_4^2 + 8a_1(a_1^2 - a_2^2 - a_3^2)a_4 + 2(a_1 - a_2 + a_3)(a_1 + a_2 + a_3)(a_1 - a_2 - a_3)(a_1 + a_2 - a_3), \quad (16)$$

$$a_4^4 + 4a_1a_4^3 + (6a_1^2 - 2a_2^2 - 4a_2a_3 - 2a_3^2)a_4^2 + 4a_1a_4(a_1 + a_2 + a_3)(a_1 - a_2 - a_3) + (a_1 + a_2 + a_3)^2(a_1 - a_2 - a_3)^2. \quad (17)$$

Now we can make the input angle generate a desired function with a measure of the transmission angle, $v_3 = f(v_1)$. We arbitrarily choose this function to be

$$v_3 \;=\; 2 + \tan\left(\frac{v_1^2}{v_1^2+1}\right), \quad (18)$$

and we arbitrarily choose a symmetric angle parameter range of

$$-2 \;\leq\; v_1 \;\leq\; 2,$$

which corresponds approximately to the angular bounds

$$-127^\circ \;\leq\; \theta_1 \;\leq\; 127^\circ.$$

The next step is childishly simple, but remarkably elegant: integrate the function array as

$$\int_{v_{1_{\min}}}^{v_{1_{\max}}} \mathbf{s}_{v_1,f(v_1)}. \quad (19)$$

The synthesis equations are obtained using two Euclidean inner products. Let the link length array be defined as

$$\mathbf{a}_{v_1,v_3}, \quad (20)$$

whose nine elements are the nine Equations (9-17). The only synthesis equation required is revealed with the numerical minimisation of Euclidean inner product

$$\min_{(a_1,a_2,a_3,a_4)\in\mathbb{R}} \left(\mathbf{a}_{v_1,v_3} \cdot \int_{v_{1_{\min}}}^{v_{1_{\max}}} \mathbf{s}_{v_1,f(v_1)} \right). \quad (21)$$

Because the least-squares optimiser used in Maple 2021 is sensitive to the quality of initial guesses, we identify the link lengths that are obtained with exact synthesis where the input angle parameters were selected as v_1 = -2, 0, 2, and the three synthesis equations generated with Eq. (4) led to the surprising result with link lengths according to a_1 is a function of a_3 and a_4, a_2 is a different function of a_3 and a_4, while a_3 and a_4 are arbitrary:

$$\left.\begin{array}{rcl} a_1 &=& f(a_3,a_4); \\ a_2 &=& g(a_3,a_4); \\ a_3 &=& a_3; \\ a_4 &=& a_4. \end{array}\right\} \quad (22)$$

For values of $a_3 = a_4 = 1$ we obtain $a_1 = 0.1878149423$ and $a_2 = 1.478438966$. Substituting these link lengths as initial guesses into the optimiser led to:

$$\left.\begin{array}{rcl} a_1 &=& 0.0905138698274517; \\ a_2 &=& 1.39186927669424; \\ a_3 &=& 0.563170358913259; \\ a_4 &=& 1.04879305299696. \end{array}\right\} \quad (23)$$

These link lengths are remarkably different from the initial guess, which is not surprising, but the arbitrariness of a_3 and a_4 is lost in the continuous approximate synthesis. Substituting these lengths into the v_1-v_3 IO equation gives

$$0.4307407243v_1^2v_3^2 - 5.483015140v_1^2 + 1.182000492v_3^2 - 4.731755372. \quad (24)$$

Fig. 3 illustrates the desired function, Eq. (18), and the one generated by the linkage implied by Eq. (24). The residual error between the desired and generated functions is

$$r \;=\; 0.00467. \quad (25)$$

According to an observation made in [22], since the cardinality of the IO data set is infinite, this linkage possesses the least design and structural errors for generating the desired function over the desired range.

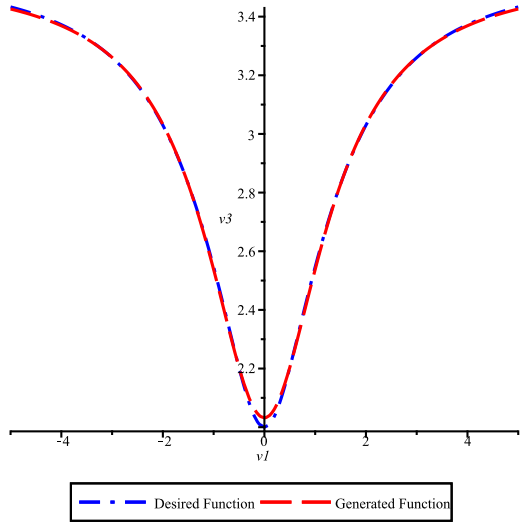

Fig. 3. Desired and generated functions $v_3 = f(v_1)$.

B. Mobility Classification

Treating each pair v_i-v_j to be coordinate axes in the plane spanned by the two, then each IO equation contains two double points at infinity on the v_i and v_j axes. The double points at infinity belonging to each of the four distinct v_i coordinate axes together with the type of points at $v_i = 0$ completely define the mobility limits, if they exist, between each v_i-v_j angle parameter pair. Physically speaking, the nature of these two points determine if extreme orientations exist that are implied by the v_i where the two links can align. Hence, the examination of these two points is sufficient to determine whether a particular joint enables a crank, a rocker, a π-rocker, or a 0-rocker link motion [20].

One possibility to determine the type of double point, i.e., whether it is a crunode, acnode, or cusp, is to evaluate whether the double point has a pair of real, or complex conjugate tangents. If the double point has two real distinct tangents, it is a crunode; if it has two real coincident tangents, it is a cusp; and if the tangents are both complex conjugates, the double point is an acnode [13], [23]. Thus, after homogenising each v_i-v_j angle pair IO equation using the homogenising coordinate w, leading to IO_h, the following discriminant yields information on the double point at infinity on the v_j axis:

$$\Delta = \left(\frac{\partial^2 IO_h}{\partial v_i \partial w}\right)^2 - \frac{\partial^2 IO_h}{\partial v_i^2}\frac{\partial^2 IO_h}{\partial w^2} \begin{cases} > 0 \Rightarrow \text{crunode;} \\ = 0 \Rightarrow \text{cusp;} \\ < 0 \Rightarrow \text{acnode.} \end{cases} \tag{26}$$

Proceeding with the double point analysis of all six v_i-v_j equations at infinity on both axes results in 12 discriminants. However, as the v_i-v_j equations are all dependent on each other, only four are distinct. Each one describes the nature of the double point at infinity of each v_i for $i \in \{1...4\}$:

$$\begin{aligned} \Delta_{v_1} &= -4(a_1 + a_2 - a_3 - a_4)(a_1 + a_2 + a_3 - a_4) \\ &\quad (a_1 - a_2 + a_3 - a_4)(a_1 - a_2 - a_3 - a_4); \end{aligned}$$

$$\begin{aligned} \Delta_{v_2} &= -4(a_1 - a_2 - a_3 + a_4)(a_1 - a_2 + a_3 + a_4) \\ &\quad (a_1 - a_2 + a_3 - a_4)(a_1 - a_2 - a_3 - a_4); \end{aligned}$$

$$\begin{aligned} \Delta_{v_3} &= -4(a_1 - a_2 + a_3 + a_4)(a_1 + a_2 - a_3 + a_4) \\ &\quad (a_1 + a_2 - a_3 - a_4)(a_1 - a_2 + a_3 - a_4); \end{aligned}$$

$$\begin{aligned} \Delta_{v_4} &= -4(a_1 + a_2 - a_3 + a_4)(a_1 - a_2 - a_3 + a_4) \\ &\quad (a_1 - a_2 + a_3 - a_4)(a_1 + a_2 + a_3 - a_4). \end{aligned}$$

Using the bilinear factors defined by Eq. (2) these discriminants can be rewritten compactly as

$$\Delta_{v_1} = -4\, A_1 A_2 B_1 B_2, \tag{27}$$
$$\Delta_{v_2} = -4\, A_1 B_2 C_1 D_2, \tag{28}$$
$$\Delta_{v_3} = -4\, A_1 B_1 C_2 D_2, \tag{29}$$
$$\Delta_{v_4} = -4\, A_1 A_2 C_1 C_2. \tag{30}$$

From these conditions we can extract the following information. If $\Delta_{v_1} \geq 0$, then the double point at $v_1 = \infty$ is either a crunode or a cusp. Knowing that $v_1 = \infty$ corresponds to $\theta_1 = 180°$, this implies that the link a_1 can physically reach the extreme position where a_1 aligns with and overlays the previous link a_4. Similarly, if $\Delta_{v_1} < 0$, then the double point at $v_1 = \infty$ is an acnode which in turn indicates that a_1 can not physically reach the extreme position where a_1 aligns with and overlays a_4. Analogous conclusions can be drawn from Equations (28), (29), and (30).

As previously mentioned, to fully understand the mobility of every link, it equally requires the analysis of whether the other extremes where the link under investigation aligns with the previous link. We need to investigate whether the linkage is assemblable at $v_i = 0$. Clearly, one possibility to obtain a condition with this information can be derived using the six v_i-v_j equations by substituting $v_i = 0$ and solving for v_j. Again, due to the equations' dependencies, we obtain four distinct conditions, one for each v_i:

$$\begin{aligned} \Omega_{v_1} &= [-(a_1 - a_2 - a_3 + a_4)(a_1 - a_2 + a_3 + a_4) \\ &\quad (a_1 + a_2 - a_3 + a_4)(a_1 + a_2 + a_3 + a_4)]^{\frac{1}{2}}; \end{aligned}$$

$$\begin{aligned} \Omega_{v_2} &= [-(a_1 + a_2 - a_3 - a_4)(a_1 + a_2 + a_3 - a_4) \\ &\quad (a_1 + a_2 - a_3 + a_4)(a_1 + a_2 + a_3 + a_4)]^{\frac{1}{2}}; \end{aligned}$$

$$\begin{aligned} \Omega_{v_3} &= [-(a_1 + a_2 + a_3 - a_4)(a_1 - a_2 - a_3 - a_4) \\ &\quad (a_1 - a_2 - a_3 + a_4)(a_1 + a_2 + a_3 + a_4)]^{\frac{1}{2}}; \end{aligned}$$

$$\begin{aligned} \Omega_{v_4} &= [-(a_1 - a_2 - a_3 - a_4)(a_1 + a_2 - a_3 - a_4) \\ &\quad (a_1 - a_2 + a_3 + a_4)(a_1 + a_2 + a_3 + a_4)]^{\frac{1}{2}}. \end{aligned}$$

Again using the bilinear factors from Eq. 2 these expressions can be rewritten compactly as:

$$\Omega_{v_1} = \sqrt{-C_1 C_2 D_1 D_2}; \tag{31}$$
$$\Omega_{v_2} = \sqrt{-A_2 B_1 C_2 D_1}; \tag{32}$$
$$\Omega_{v_3} = \sqrt{-A_2 B_2 C_1 D_1}; \tag{33}$$
$$\Omega_{v_4} = \sqrt{-B_1 B_2 D_1 D_2}. \tag{34}$$

With this information we can establish a completely generic classification scheme to determine the relative mobilities of every link in the simple closed kinematic chain. Using the bilinear factors the classification can be constructed according to Tables II-V. The beauty of this classification scheme lies in its completely generic nature, covering both positive and negative values for the a_i. This result requires the a_i to be considered as directed line segments. For example $a_1 > 0$ means that it is directed from the join with a_4 to a_2, $a_1 < 0$ means a_1 points in the opposite direction. Moreover, the classification scheme is directly linked to the algebraic IO equations. We are now able to explain the different spatial sections that are spanned by the linear factors in the design parameter space reported in [20].

TABLE II

MOBILITY OF a_1 RELATIVE TO a_4.

$A_1A_2B_1B_2$	$C_1C_2D_1D_2$	mobility of a_1
≤ 0	≤ 0	crank
$\not\leq 0$	> 0	π-rocker
> 0	≤ 0	0-rocker
> 0	> 0	rocker

TABLE III

MOBILITY OF a_2 RELATIVE TO a_1.

$A_1B_2C_1D_2$	$A_2B_1C_2D_1$	mobility of a_2
≤ 0	≤ 0	crank
$\not\leq 0$	> 0	π-rocker
> 0	≤ 0	0-rocker
> 0	> 0	rocker

TABLE IV

MOBILITY OF a_3 RELATIVE TO a_2.

$A_1B_1C_2D_2$	$A_2B_2C_1D_1$	mobility of a_3
≤ 0	≤ 0	crank
$\not\leq 0$	> 0	π-rocker
> 0	≤ 0	0-rocker
> 0	> 0	rocker

TABLE V

MOBILITY OF a_4 RELATIVE TO a_3.

$A_1A_2C_1C_2$	$B_1B_2D_1D_2$	mobility of a_4
≤ 0	≤ 0	crank
$\not\leq 0$	> 0	π-rocker
> 0	≤ 0	0-rocker
> 0	> 0	rocker

C. Design Parameter Space

The literature provides several geometric mobility interpretations for planar four bar linkages in different design parameter spaces. For example, Gosselin and Angeles defined mobility regions in a 3D space spanned by the Freudenstein parameters [24]. A *solution space* spanned by the link length ratios of $\lambda_1 = a_4/a_1$, $\lambda_3 = a_2/a_1$ and $\lambda_4 = a_3/a_1$ in which Grashof and non-Grashof linkages are identified is described in [25].

We will, however, build upon the design parameter representation from [20] which considers the bilinear factors from Eq. (2) in the parameter space spanned by a_1, a_2 and a_3 whose points represent normalised four bar linkages with base lengths of $a_4 = 1$. Considered as planes, the eight bilinear factors intersect in the edges of a uniform double tetrahedron and completely represents the input and output mobility of planar four bar linkages, see Fig. 4 (a). The spherical 4R IO equations contain eight bi-cubic surfaces which, together, contain 12 real lines containing segments that are the edges of a topologically identical double tetrahedron [16], see Fig. 5.

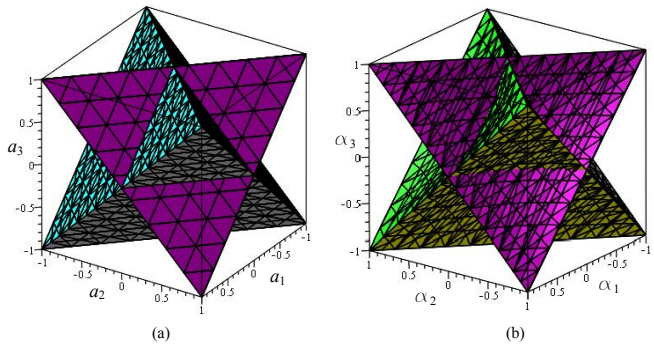

Fig. 4. Design parameter space surfaces: (a) planar 4R; (b) spherical 4R.

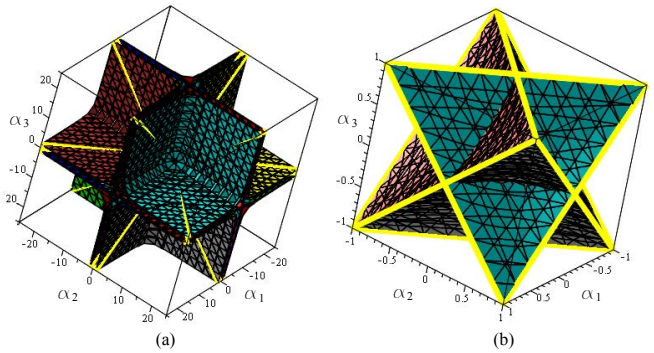

Fig. 5. 12 distinct lines, three on each of eight cubics: (a) zoomed out; (b) zoomed in.

With the six algebraic v_i-v_j equations, and the previously identified mobility classification using double points and discriminants, it becomes evident that the planes containing the faces of the double tetrahedron contain even more mobility information than stated in [20], namely, information on the mobility of every link in the chain! In fact, the double tetrahedron face planes segment the design parameter space into distinct regions which each describes the mobility of a_1, a_2, a_3 and a_4. Since a complete analysis of the design parameter space would go beyond the scope of this paper, we will limit the discussion herein to one short example as follows.

Consider the intersection traces of the bilinear factors in the parameter plane $a_1 = 0.5$ spanned by a_2 and a_3 in the design parameter space. Here the bilinear factors are parallel and orthogonal lines. Together with Tables II-V, the mobility of all a_2 and a_3 of any length can now be identified, resulting

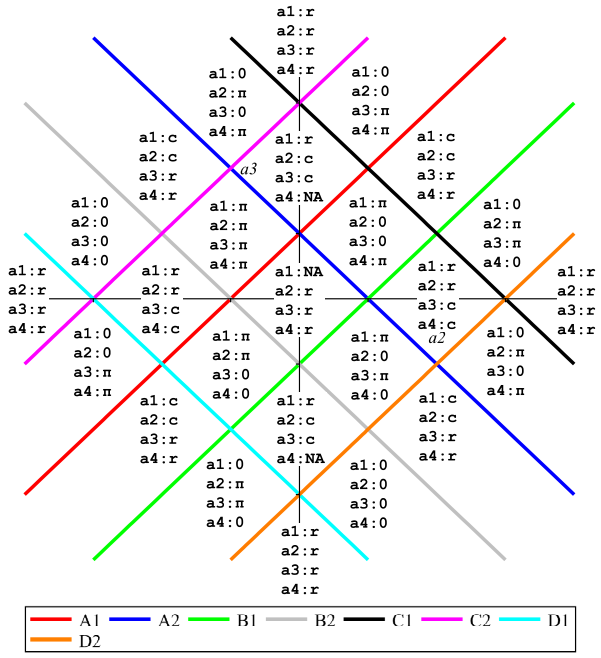

Fig. 6. Intersection of the double tetrahedron in the design parameter space with the plane $a_1 = 0.5$.

in Fig. 6 where **r** indicates that the corresponding link is a rocker, **c** a crank, π a π-rocker, and **0** a 0-rocker, while NA indicates not assemblable. This analysis can be conducted for every area separated by the bilinear factors in the design parameter space, resulting in a complete geometric mobility classification of planar four bar linkages which is directly linked to the six algebraic v_i-v_j equations.

IV. CONCLUSIONS

The importance of the work is nicely summarised by the example applications to mobility classification, the design parameter space, and continuous approximate synthesis. The obvious extension to this work is to identify a way to perform optimal dimensional synthesis to specify more than one function for a planar 4R linkage to generate between different angle pairs. Because the location of a linkage in the design parameter space determines the mobility of the particular linkage and determines the six distinct functions $v_j = f(v_i)$, it may be possible to specify six desired functions and then to identify the link lengths that generate all six with the least residual error.

REFERENCES

[1] M. Ceccarelli, Ed., *Distinguished Figures in Mechanism and Machine Science, Their Contributions and Legacies Part 1.* Springer, New York, U.S.A., 2007.

[2] R. S. Hartenberg and J. Denavit, *Kinematic Synthesis of Linkages*. McGraw-Hill Book Co., New York, N.Y., U.S.A., 1964.

[3] H. Schröcker, M. Husty, and J. McCarthy, "Kinematic Mapping Based Evaluation of Assembly Modes for Planar Four-Bar Synthesis," *ASME, Journal of Mechanical Design*, vol. 129, no. 9, pp. 924–929, 2007.

[4] S. Bai and J. Angeles, "A Unified Input–output Analysis of Four-bar Linkages," *Mechanism and Machine Theory*, vol. 43(2), pp. 240–251, 2008.

[5] T. S. Todorov, "Synthesis of Four Bar Mechanisms as Function Generators by Freudenstein-Chebyshev." *Journal of Robotics and Mechanical Engineering Research*, vol. 1(1), 2015.

[6] S. Deshpande and A. Purwar, "A Machine Learning Approach to Kinematic Synthesis of Defect-free Planar Four-bar Linkages," *Journal of Computing and Information Science in Engineering*, vol. 19(2), 2019.

[7] Q. J. Ge, Purwar, A., Zhao, P., and S. Deshpande, "A Task-Driven Approach to Unified Synthesis of Planar Four-Bar Linkages Using Algebraic Fitting of a Pencil of G-Manifolds," *Journal of Computing and Information Science in Engineering*, vol. 17(3), 2019.

[8] R. Wu, R. Li, and S. Bai, "A Fully Analytical Method for Coupler-curve Synthesis of Planar Four-bar Linkages," *Mechanism and Machine Theory*, vol. 155, 2021.

[9] J. Denavit and R. S. Hartenberg, "A Kinematic Notation for Lower-pair Mechanisms Based on Matrices," *Trans ASME J. Appl. Mech.*, vol. 23, p. 215–221, 1955.

[10] E. Study, *Geometrie der Dynamen*. Teubner Verlag, Leipzig, Germany, 1903.

[11] F. Klein, *Elementary Mathematics from an Advanced Standpoint: Geometry*. Dover Publications, Inc., New York, N.Y., U.S.A., 1939.

[12] O. Bottema and B. Roth, *Theoretical Kinematics*. Dover Publications, Inc., New York, N.Y., 1990.

[13] M. L. Husty, A. Karger, H. Sachs, and W. Steinhilper, *Kinematik und Robotik*. Springer-Verlag, Berlin, Germany, 1997.

[14] D. Cox, J. Little, and D. O'Shea, *Ideals, Varieties, and Algorithms: an Introduction to Computational Algebraic Geometry and Commutative Algebra,* second edition. Springer-Verlag, Berlin, Germany, 1997.

[15] M. Rotzoll, M. J. D. Hayes, M. L. Husty, and M. Pfurner, "A General Method for Determining Algebraic Input-output Equations for Planar and Spherical 4R Linkages." Advances in Robotic Kinematics 2020, eds. Lenarčič, J. and Parenti-Castelli, V., Springer Nature Switzerland AG, Cham, Switzerlnd, 2020, pp. 96–97.

[16] M. Hayes, M. Rotzoll, C. Ingalls, and M. Pfurner, "Design Parameter Space of Spherical Four-bar Linkages." New Trends in Mechanism and Machine Science, EuCoMeas, eds. Pisla, D., Corves, B., and Vaida, C., Springer Nature Switzerland AG, Cham, Switzerlnd, 2020, pp. 19–27.

[17] M. Rotzoll and M. J. D. Hayes, "A General Method for Determining Algebraic Input-output Equations for the Slider-crank and the Bennett Linkage." 11th CCToMM Symposium on Mechanisms, Machines, and Mechatronics, eds. S. Nokleby, and P. Cardou, Ontario Tech University, Oshawa, ON, Canada, June 3-4, 2021.

[18] E. J. F. Primrose, *Plane Algebraic Curves*. MacMillan, 1955.

[19] W. Adams and P. Loustaunau, *An Introduction to Gröbner Bases*. American Mathematical Society, Graduate Studies in Mathematics, 1994, vol. 3.

[20] M. J. D. Hayes, M. Rotzoll, and M. L. Husty, "Design Parameter Space of Planar Four-bar Linkages," in *Advances in Mechanisms and Machine Science,* Springer, Cham, vol. 73, 2019, pp. 229–238.

[21] Z. Copeland, M. Rotzoll, and M. J. D. Hayes, "Concurrent Type and Dimensional Continuous Approximate Function Generator Synthesis for All Planar Four-bar Mechanisms." 11th CCToMM Symposium on Mechanisms, Machines, and Mechatronics, eds. S. Nokleby, and P. Cardou, Ontario Tech University, Oshawa, ON, Canada, June 3-4, 2021.

[22] M. J. D. Hayes, K. Parsa, and J. Angeles, "The Effect of Data-Set Cardinality on the Design and Structural Errors of Four-Bar Function-Generators," *Proceedings of the Tenth World Congress on the Theory of Machines and Mechanisms,* Oulu, Finland, pp. 437–442, 1999.

[23] R. Cipolla and P. Giblin, *Visual Motion of Curves and Surfaces*. Cambridge University Press, Cambridge, U.K., 2000.

[24] C. M. Gosselin and J. Angeles, "Optimization of Planar and Spherical Function Generators as Minimum-defect Linkages," *Mechanism and Machine Theory*, vol. 24, no. 4, pp. 293–307, 1989.

[25] C. R. Barker, "A Complete Classification of Planar of Four-bar Linkages," *Mechanism and Machine Theory*, vol. 26, no. 6, pp. 535–554, 1995.